

# Antibody Repertoire of Human Polyclonal Antibodies Against Ebola Virus Glycoprotein Generated After Deoxyribonucleic Acid and Protein Vaccination of Transchromosomal Bovines

Sandra Fuentes, Supriya Ravichandran, and Surender Khurana

Division of Viral Products, Center for Biologics Evaluation and Research, US Food and Drug Administration, Silver Spring, Maryland

Several Ebola vaccines and therapeutics are under clinical development. However, limited knowledge exists on the quality of antibody response generated by different Ebola vaccines. In this study, antibody repertoire induced by vaccination of transchromosomal bovine (TcB) with Ebola virus (EBOV) glycoprotein ([GP]; recombinant GP [rGP]) encoded by either deoxyribonucleic acid (DNA) or nanoparticle-based vaccine platform was analyzed using EBOV genome fragment phage display library and surface plasmon resonance (SPR)-based real-time kinetics assay to measure antibody affinity maturation to both native and partially denatured Ebola GP as well as GP containing the receptor binding domain but lacking the mucin-like domain. Immunoglobulin (IgG) obtained from rGP nanoparticle-vaccinated TcB demonstrated ~4-fold higher binding affinity compared with DNA-vaccinated TcB-induced IgG against the native rGP's. The rGP nanoparticle vaccine generated a more robust and diverse antibody immune response to the native EBOV-GP compared with the DNA vaccine, which may explain the protective efficacy observed for these antibody preparations.

**Keywords.** antibody; Ebola; gene fragment phage display library; surface plasmon resonance; vaccine.

The Ebola virus (EBOV) outbreak in Western Africa led to renewed efforts to develop a vaccine and/or therapeutics to provide protection against severe EBOV disease (EVD). Most vaccine candidates target the glycoprotein (GP) of the EBOV, because anti-GP antibodies demonstrated protection against EVD in animal models [1–3]. SAB Biotherapeutics (SAB) has developed a transchromosomal bovine (TcB) in which the bovine immunoglobulin (Ig) genes have been knocked out and a human artificial chromosome containing the full germ-line sequence of human Ig has been inserted, allowing the TcB to produce target-specific fully human antibodies after vaccination [4, 5]. This animal model rapidly produces large quantities of polyclonal human IgGs, which can be used for passive prophylaxis against pathogens, thus reducing the risk of an adverse reaction in humans. In a recent study, 2 TcB human IgGs were investigated in human clinical trials for Middle East respiratory syndrome coronavirus [6] and *Mycoplasma hominis* indications (termed SAB-301 and SAB-136, respectively). SAB-301 was safe and well tolerated in a completed phase I clinical trial with an average terminal IgG elimination half-life ( $t_{1/2}$ ) of ~28 days that is similar to human-derived intravenous Ig [7]. SAB-136 was safe and efficacious in a phase I clinical trial that treated a patient

with severe immunodeficiency, hypogammaglobinemia, and multiyear chronic *M hominis* septic hip and polyarthritis. The patient received SAB-136 for 1 year, and the drug was well tolerated with no significant adverse events and displayed improved clinical parameters with decreased mycoplasma burden [8]. Previously, a codon optimized EBOV GP deoxyribonucleic acid (DNA) vaccine and a recombinant GP (rGP) nanoparticle vaccine were used to immunize TcB that resulted in production of EBOV GP neutralizing antibodies, which provided partial protection in mice when passively administered after lethal EBOV challenge [9, 10]. However, better understanding of the polyclonal antibody repertoire and antibody quality generated after different vaccine platforms is critical for further development and evaluation of effective EBOV vaccine candidates and therapeutic antibody preparations. In this study, a comprehensive analysis of the humoral immune response induced by 2 different vaccine platforms in the TcBs was evaluated.

## METHODS

### Transchromosomal Bovine Human Polyclonal Antibodies

The production of fully human Ig from TcB has been described previously [4]. Purified polyclonal human antibody lot nos. SAB-132 and SAB-139 were a gift from SAB. Polyclonal human antibody lot no. SAB-132 was obtained from TcBs, immunized 3 times at intervals of 3–4 weeks with 10 mg of codon-optimized plasmid DNA encoding EBOV GP and 10 mg of plasmid DNA encoding Sudan ebolavirus (SUDV) GP (EBOV/SUDV GP) by intramuscular electroporation [9]. Human polyclonal

Correspondence: S. Khurana, PhD, Division of Viral Products, Center for Biologics Evaluation and Research, US Food and Drug Administration, 10903 New Hampshire Avenue, Silver Spring, MD 20903 (surender.khurana@fda.hhs.gov).

The Journal of Infectious Diseases® 2018;218(S5):S597–602

Published by Oxford University Press for the Infectious Diseases Society of America 2018. This work is written by (a) US Government employee(s) and is in the public domain in the US. DOI: 10.1093/infdis/jiy325

GP antibody lot no. SAB-139 is the product of TcBs vaccinated thrice with 2 mg/kg rGP nanoparticles [10]. Fully human IgGs (SAB-132 and SAB-139) induced after TcB immunization were purified as described before [9, 10].

#### **Construction of Ebola Glycoprotein Gene-Fragment Phage Display Library and Affinity Selection by Panning**

Construction of the gene-fragment phage display library for the complete EBOV GP was previously described [11]. Gene-fragment phage display library (GFPDL) was constructed using the entire EBOV GP and can potentially display all possible viral protein segments from 15 to 330 amino acids, as fusion protein on the surface of bacteriophage. Before GFPDL panning with purified IgG (SAB-132 and SAB-139), polyclonal antibodies were incubated with ultraviolet-killed M13K07 to remove antibodies, which can nonspecifically interact with phage proteins. Subsequent GFPDL affinity selection was carried out in solution (with Protein A/G) using 1 mg of preadsorbed IgG from each of SAB-132 and SAB-139 as previously described [11–13].

#### **Real-Time Antibody Kinetic Analysis of Transchromosomal Bovine Immunoglobulin G to Recombinant Glycoprotein Proteins and Off-Rate Measurements by Surface Plasmon Resonance**

Steady-state equilibrium binding of DNA and rGP-vaccinated TcB IgG lot SAB-132 and SAB-139, respectively, was monitored at 25°C using a ProteOn surface plasmon resonance ([SPR] Bio-Rad). Recombinant GP (1–650 residues) and rGP-N-terminal half containing receptor binding domain ([RBD] 1–308 residues) were expressed fused to a polyhistidine tag at the C-terminus and purified using Ni-NTA chromatography. The EBOV-GP proteins were coupled to a GLC sensor chip with amine coupling at pH 4.5 (partial denaturing condition) with 100 resonance units (RUs), or they were captured on an HTG surface (native condition) via the His<sub>6</sub> tag at 100 RUs in the test flow cells. Samples of 200- $\mu$ L serially diluted purified SAB-132 and SAB-139 at 1, 0.1, and 0.01 mg/mL were injected at a flow rate of 50  $\mu$ L/minute (240-second contact time) for association, and dissociation was performed over a 1200-second interval (at a flow rate of 50  $\mu$ L/minute). Responses from the protein surface were corrected for the response from a mock surface and for responses from a separate, buffer-only injection. Monoclonal antibody (MAb) 2D7 (anti-CCR5) was used as a negative control in these experiments. Antibody off-rate constants, which describe the stability of the complex, ie, the fraction of complexes that decays per second, were determined directly from the SAB-132 and SAB-139 polyclonal IgG interaction with rGP using SPR (as described above) and calculated using the Bio-Rad ProteOn manager software for the heterogeneous sample model as previously described [11, 13]. To improve the measurements, the off-rate constants were determined from 2 independent SPR runs.

Antigenic site peptides V.8 (394–405) and V.9 (399–414) were synthesized using F-moc chemistry and conjugated to Biotin at the carboxy terminus. Biotinylated peptides were captured on a NLC Chip (Bio-Rad) to saturation, and SAB-132 and SAB-139 antibody binding was evaluated by SPR as per the experimental conditions described above.

## **RESULTS**

#### **Antibody Epitope Repertoire After Deoxyribonucleic Acid and Recombinant Glycoprotein Nanoparticle Immunization**

To analyze the diversity of antibody epitope profile induced by the 2 vaccine strategies, plasma from TcBs immunized 3 times with codon optimized EBOV GP DNA or a rGP nanoparticle vaccine were collected and purified for fully human IgG [9, 10]. These IgG preparations were evaluated using a highly diverse EBOV GP GFPDL library ( $>10^7$  unique phage clones) composed of GP fragments spanning the entire GP that was previously used for analyzing human antibody response to live rVSV $\Delta$ G-ZEBOV-GP vaccination in adults [11]. The GFPDL affinity selection showed that the prevaccination IgG (negative control) bound very few phages across most of the GP (data not shown). SAB-139 (rGP nanoparticle vaccinated animals) purified IgG demonstrated 2-fold higher number of phages bound compared with the SAB-132 (DNA vaccinated animals) IgG. Sequencing of GP fragments expressed by eluted phages showed a high frequency of phage displayed peptides mapping across the GP1 head domain and the C-terminal GP2 stalk domain of the EBOV GP (Figure 1A and B). Both SAB-132 and SAB-139 bound phages containing GP sequences predominantly from the glycan cap and the mucin-like domains (MLDs). However, rGP nanoparticle-generated SAB-139 antibodies showed more diverse antibody epitope profile than the DNA vaccine-generated SAB-132 IgG. Specifically, SAB-139 recognized more epitopes mapping to the C-terminus of GP1 and to the heptad repeat 2 in GP2 stalk domain.

#### **Frequency and Distribution of Antigenic Sites Within Ebola Glycoprotein Recognized by Antibodies After Deoxyribonucleic Acid and Recombinant Glycoprotein Nanoparticle Vaccination**

In a previous study, we identified 19 antigenic regions/sites (represented with gray bars in Figure 1C and D) in the EBOV GP induced by a live rVSV $\Delta$ G-ZEBOV-GP vaccine in humans [11]. The EBOV/SUDV-GP DNA (SAB-132) and rGP nanoparticle (SAB-139) vaccination of TcBs induced antibodies that identified 6 additional antigenic sites in the current study (represented with black bars in Figure 1C and D); site IV.4 is in the glycan cap, and sites IV.5–IV.7 and V.8–V.9 are located in the MLD of EBOV-GP. The frequency of the antibody captured phage clones displaying these 25 antigenic sites by SAB-132 and SAB-139 antibodies was evaluated. No antibodies bound to previously described antigenic regions I, II, III, IV, and V or antigenic sites II.1, III.1, and V.3 (represented by gray bars with gray

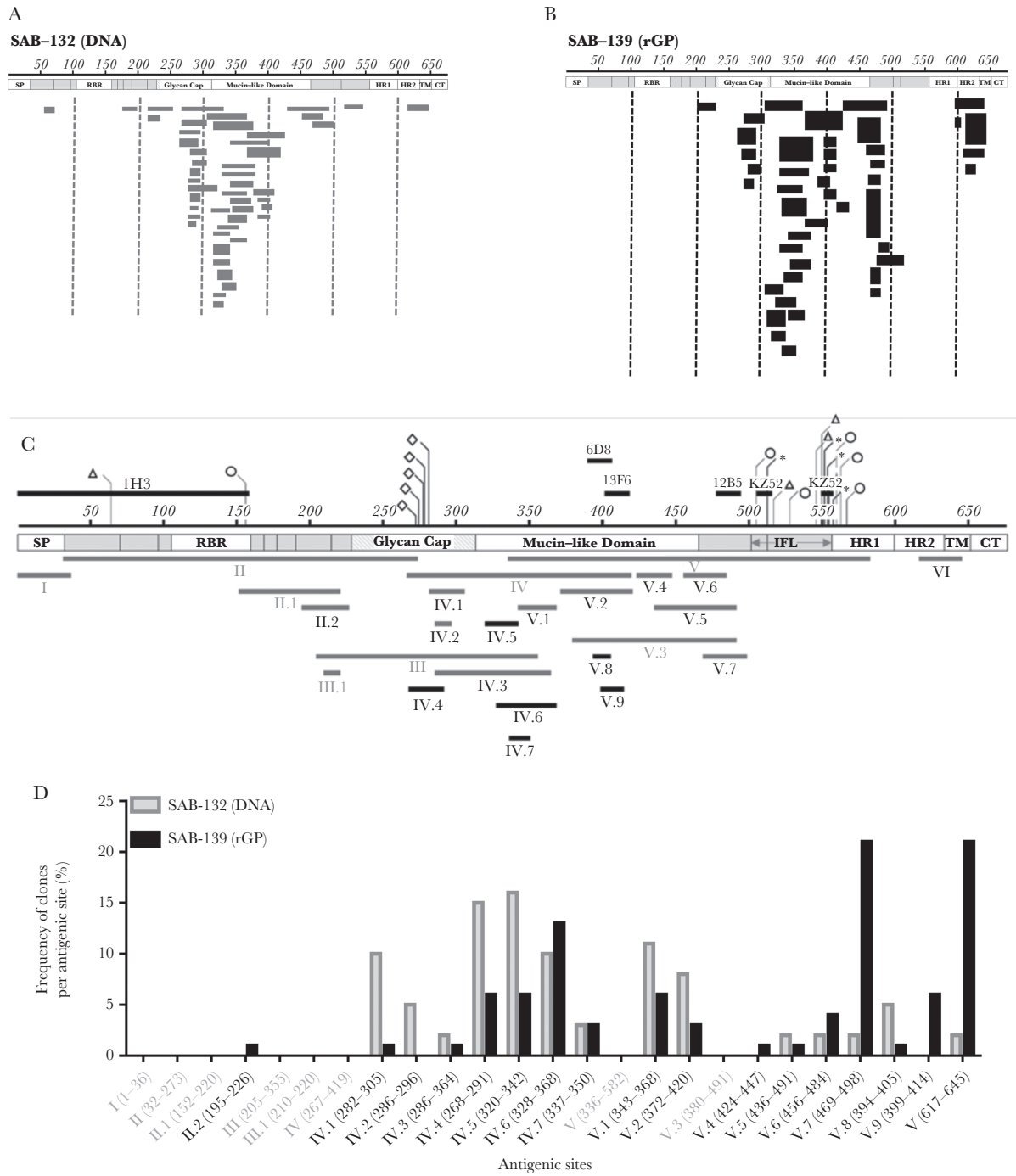


**Figure 1.** Evaluation of antibody epitope repertoire induced in transchromosomal bovine (TcB) after vaccination with Ebola virus (EBOV)/Sudan ebolavirus (SUDV) glycoprotein (GP) deoxyribonucleic acid (DNA) or EBOV GP nanoparticle. (A and B) Distribution of phage clones after GP-genome fragment phage display library (GFPDL) affinity selection with purified immunoglobulin G from TcB after 3 immunizations with (A) EBOV/SUDV-GP DNA (SAB-132) or (B) EBOV GP nanoparticle (SAB-139) vaccine. The amino acid number designation is based on the EBOV-Mayinga GP sequence. Bar position and length indicates the identity of the displayed GP protein sequence on the phage clones after affinity selection. The thickness of each bar represents the frequencies of repetitively isolated phage inserts. (C) Schematic representation of antigenic sites in the EBOV GP. Previously described monoclonal antibody (MAb) binding sites are shown above, and the antigenic sites evaluated in this study are depicted below the GP protein graphic. Critical residues for binding of MAbs in anti-EBOV cocktails ZMAb (1H3, 2G4, and 4G7; shown as asterisks), MB-003 (13C6 [shown as diamonds], 6D8, and 13F6), fusion loop-specific antibodies; CA45 (shown as triangles), ADI-15742/15878 (shown as circles), and MAb KZ52 are depicted. Antigenic sites identified previously are represented by gray bars [11]; new antigenic sites are in black bars. Previously identified antigenic sites represented by gray bars and gray letters had a frequency of <1% in this study. The sites identified in the current study are shown in black letters. (D) Frequency of phage clones expressing each of the EBOV-GP antigenic sites. The number of clones that coded for each antigenic site was divided by the total number of EBOV-GFPDL clones eluted for each sample and represented as a percentage. Abbreviations: CT, cytoplasmic tail; HR1, heptad repeat 1; HR2, heptad repeat 2; RBR, receptor binding region; rGP, recombinant GP; SP, signal peptide; TM, transmembrane domain.

letters in Figure 1C) that were recognized by antibodies induced by a live rVSVΔG-ZEBOV-GP vaccine in humans [11]. The EBOV/SUDV GP DNA vaccine (SAB-132) induced a higher frequency of antibodies that bound primarily to antigenic sites IV.1, IV.2, IV.4, and IV.5 in the GP glycan cap and V.1 and V.2 in the MLD. The rGP vaccine (SAB-139) induced antibodies that predominantly recognized antigenic sites IV.6 in the MLD, V.7 and V.9 in the C-terminus of GP1, and site VI in GP2. Taken together, the results from the EBOV-GP GFPDL affinity selection showed that the rGP nanoparticle vaccine induced a more diverse antibody repertoire than the DNA vaccine, and the antibodies recognized a wider range of epitopes in the EBOV GP.

#### Glycoprotein Nanoparticle Vaccine Promotes Robust Antibody Response to Native Conformational Recombinant Glycoprotein Compared With Deoxyribonucleic Acid Vaccination

Surface plasmon resonance assay was optimized to analyze polyclonal antibody association and dissociation kinetics, which reflects the overall antibody binding avidity [11]. In previous studies, SPR using His<sub>6</sub>-tag captured protein on HTG

chips with a panel of conformation-dependent GP-specific neutralizing MAbs confirmed conservation of native GP structure. However, these MAbs lost binding to rGP that was amine-coupled directly to GLC chips, suggesting partial denaturation of the GP and loss of conformational epitopes [11]. The negative control-purified TcB IgG showed very low reactivity (<5 RU at 1 mg/mL total IgG concentration) to rGPs in SPR. SAB-139 (rGP nanoparticle-induced IgG) showed 2-fold higher binding to native homologous EBOV rGP compared with SAB-132 (DNA vaccine-induced IgG) (Figure 2A). Binding of these 2 antibody preparations was also evaluated to the N-terminal half of GP (1–308 residues) containing the RBD (GP-RBD) and lacking the highly glycosylated MLD. Surface plasmon resonance antibody analysis showed that antibody binding for both SAB-132 and SAB-139 IgG to the GP-RBD was >3-fold lower than binding to complete rGP ectodomain, confirming the GFPDL analysis (Figure 1) that the majority of the antibodies after vaccination in these 2 IgG preparations recognized epitopes primarily in MLD. The 2 IgG preparations showed equivalent antibody binding levels to the partially denatured

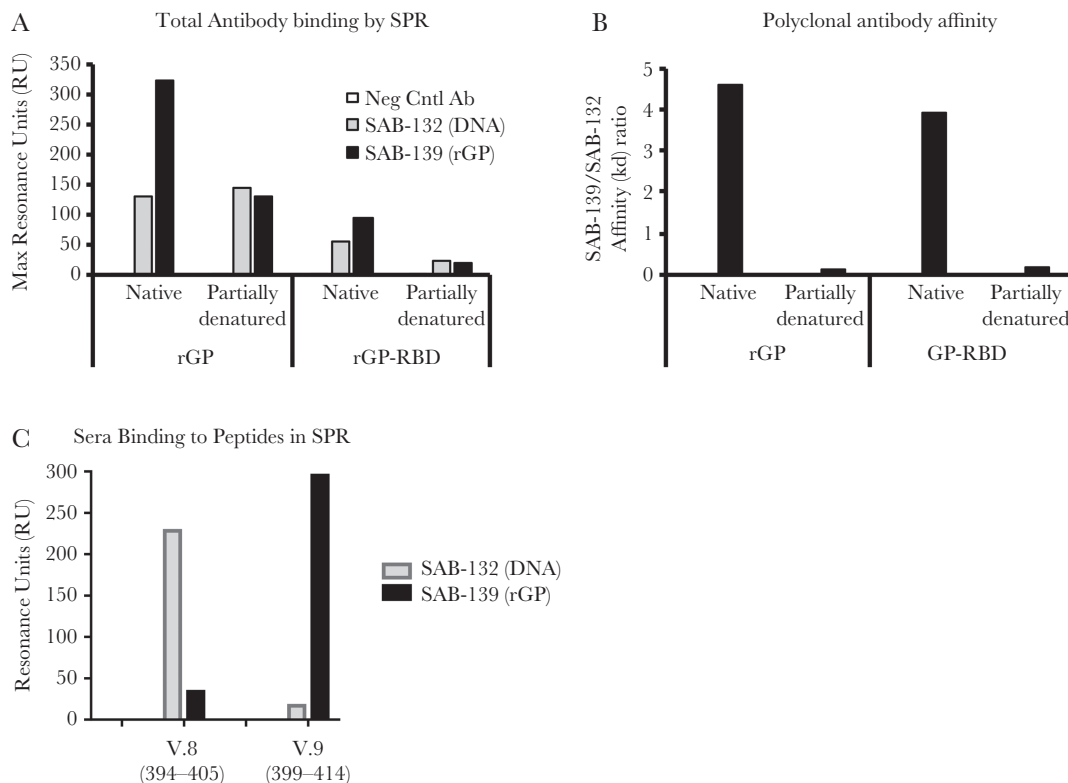


**Figure 2.** Surface plasmon resonance (SPR)-based analysis of purified human immunoglobulin G (IgG) from glycoprotein (GP) deoxyribonucleic acid (DNA) or nanoparticle-vaccinated transchromosomal bovines (TcBs) to Ebola virus (EBOV)-GP purified proteins. (A) Steady-state equilibrium analysis of the binding of TcB IgG preparations to different recombinant GP (rGP) proteins was measured under native conditions (rGP proteins immobilized on a HTG sensor chip) or under partial denaturing conditions (GLC sensor chip with amine coupling at pH 4.5). Total binding of antibodies to EBOV-GP and N-terminal half of GP (1–308 residues; GP-receptor binding domain [RBD]) containing RBD is shown. (B) Antibody affinity (off-rate constants) to rGP or GP-RBD were determined under native and partially denatured conditions. Affinity ( $K_D$ ) ratios of antibody binding induced by rGP nanoparticle (SAB-139) and EBOV/Sudan ebolavirus DNA (SAB-132) vaccine to native (left column) or partially denatured rGP (right column) shown are calculated by dividing the  $K_D$  of SAB-139 by  $K_D$  of SAB-132 for antibody binding to native or partially denatured rGP, separately. (C) Binding antibodies to antigenic site peptides, V.8 (394–405) and V.9 (399–414), using SAB-132 and SAB-139 in SPR.

rGP's, suggesting that the rGP nanoparticle-induced antibodies (SAB-139) recognized conformation-dependent epitopes that were sensitive to partial denaturation in this SPR binding assays (Figure 2A). However, the EBOV/SUDV DNA vaccine-generated antibodies (SAB-132) recognized nonconformational/linear epitopes that were not impacted by low pH-mediated denaturation in the SPR assay.

To further investigate whether the 2 vaccine platforms promote differential antibody affinity maturation and lead to an increase in antibody avidity, we determined the off-rate constants of the 2 TcB-purified IgG after binding to the native EBOV rGP and GP-RBD. We compared antibody binding off-rates to native rGP with the binding to partially denatured rGP to distinguish binding to conformational versus linear/denatured epitope-specific antibodies. SAB-139 IgG (obtained from rGP nanoparticle vaccinated TcB) demonstrated ~4-fold higher binding affinity (with slower dissociation rate constants of  $< 10e-3$  per second) compared with SAB-132 (DNA-vaccinated TcB) against the native EBOV rGP ectodomain or the GP-RBD (Figure 2B). That difference in antibody affinity between SAB-132 and SAB-139 was highly diminished when partially denatured rGPs were used, confirming that the high-affinity binding of SAB-139 IgG after GP nanoparticle immunization was primarily due to conformational-dependent epitope-specific antibodies, whereas the DNA-vaccinated SAB-132 antibodies have higher level of antibodies specific for linear/denatured epitopes in EBOV GP.

Furthermore, SPR was performed using the antigenic site peptides V.8 (394–405) and V.9 (399–414) to confirm that SAB-132 and SAB-139 possessed binding antibodies to overlapping V.8 and V.9 antigenic sites that are recognized by MAbs 6D8 and 13F6 (contained in the MB-003 cocktail), respectively. As shown in Figure 2C, SAB-132 antibodies preferentially bound site V.8, whereas SAB-139 antibodies exhibited higher binding to antigenic site V.9 peptide.

## DISCUSSION

A strong humoral immune response after vaccination has been shown to decrease disease severity and increase survival rate in EBOV animal challenge studies [2, 3, 14]. However, the efficacy of humoral immune response after vaccination against EBOV depends on the vaccine platforms and the animal models used in such studies. Understanding the immune correlates of protection against EBOV is essential for the development of an effective vaccine as well as antibody-based therapeutics. Several MAbs, polyclonal antibody preparations, and convalescent sera from nonhuman primates (NHPs) and humans have shown variable efficacy in different EBOV animal model challenge studies. KZ52 is an example of a MAb that controls infection in a small animal model but not in NHPs [15, 16]. Cocktails of MAbs or polyclonal antibodies have been developed to increase the breadth of protection that can be passively transferred with the goal of decreasing EVD severity.

Transchromosomal bovines have recently been developed to produce large quantities of human IgGs that can be used for passive immunization against various pathogens including EBOV [4, 5, 9, 10].

In this study, we performed a comprehensive analysis of polyclonal antibody response induced by 2 different vaccine platforms in the TcBs. The rGP based nanoparticle vaccine (SAB-139) induced more diverse GP-specific antibody repertoire than the EBOV/SUDV DNA-encoded GP vaccine (SAB-132) as determined by unbiased GFPDL approach. Although both vaccines induced similar antibody epitope profiles in the glycan and MLD, which has been previously identified to be recognized by some protective MAbs, the antibodies induced by the rGP vaccine recognized more antigenic sites of the EBOV GP, which could potentially include more, so far unknown, protective epitopes within these antigenic sites. The DNA vaccine-induced antibodies that recognized antigenic site V.8, which includes the epitope of protective antibody 6D8 [17, 18], whereas the rGP vaccine-induced antibodies that bound antigenic site V.9, which includes the known epitope of protective MAb 13F6 [18]. To compare the amounts of antibodies against these V.8 (394–405) and V.9 (399–414) site epitopes identified using GFPDL, SPR was performed with respective synthetic peptides. SAB-132 and SAB-139 binding profile against the 2 peptides (V.8 and V.9) demonstrated differential recognition of epitopes of these antibody preparations for the 2 overlapping antigenic sites. However, neither of the vaccines generated significant binding antibodies to the fusion loop of GP that is recognized by the anti-pan ebolavirus antibodies, CA45, ADI-15742, and ADI-15878 [19, 20]. Because the DNA vaccine contains both EBOV and SUDV GP-encoding sequence in the plasmid, it is possible that DNA vaccination induced antibodies in the SAB-132 IgG preparation recognizing the common conserved epitopes of Zaire and Sudan EBOV GP in the glycan cap region (residues 282–305) [11]. However, DNA vaccination did not induce significant binding antibodies in GP2 region that have high sequence conservation between EBOV and SUDV.

This suggests, based on results from previous animal studies, that the antibodies induced by both vaccine strategies could result in protection from severe EVD. However, the antibody epitope diversity induced by these DNA and protein-based vaccines in TcBs are considerably constrained compared with the antibody repertoire induced by the live rVSVΔG-ZEBOV-GP vaccination in adults [11], which could be due to the difference among the vaccines used in TcBs and humans as well as different vaccination hosts.

The antibody kinetics analysis by SPR demonstrated that the rGP-based nanoparticle vaccine (SAB-139) induced higher titer of native GP-specific conformation-dependent antibodies than the DNA vaccine (SAB-132) per milligram of polyclonal IgG. The difference in antibody response was not only quantitative but also qualitative. Antibody affinity after nanoparticle

vaccination to native GP was 4-fold higher compared with the DNA vaccine-induced antibodies. However, this trend was specific for affinity to the native GP, because the antibody affinity to the denatured form of GP was higher for DNA vaccine-induced IgG compared with the nanoparticle protein-based vaccine. These findings may suggest differences in processing of the native intact GP nanoparticle and DNA-encoded GP expression in host cells after immunization by the TcB immune system. The level of GP expression/secretion in vivo, after plasmid DNA vaccination, cannot be easily determined. Furthermore, the 2 vaccine platforms may also differ in the levels of CD4<sup>+</sup> T helper cells and T-follicular helper (Tfh) cells induced. The Tfh play an important role in antibody affinity maturation in germinal centers. In BALB/c mice challenge studies with mouse-adapted (ma) EBOV strain, 7 of 10 mice treated with the 100 mg/kg SAB-132 (V3) IgG and 9 of 10 mice treated with 100 mg/kg SAB-139 (V2) IgG intraperitoneally 1 day postchallenge survived the lethal EBOV infection [9, 10]. The greater antibody epitope diversity and antibody affinities observed for the SAB-139 (rGP vaccine) compared with SAB-132 (DNA vaccine) may explain the better in vitro neutralization as well as in vivo protective efficacy observed for the SAB-139 IgG preparation in the previous mice challenge studies [9, 10].

## CONCLUSIONS

Therefore, based on these findings, it is critical to develop appropriate assays that can provide better in-depth understanding of antibody responses to help guide development and evaluation of effective Ebola countermeasures including therapeutics and vaccines.

## Notes

**Disclaimer.** The funders had no role in study design, data collection and analysis, decision to publish, or preparation of the manuscript. The content of this publication does not necessarily reflect the views or policies of the Department of Health and Human Services, nor does mention of trade names, commercial products, or organizations imply endorsement by the US Government.

**Acknowledgments.** We thank Hana Golding and Keith Peden for their insightful review of the manuscript. We thank Jin-an Jiao, Eddie Sullivan, and Hua Wu (from SAB Biotherapeutics) and Thomas Luke (from Naval Medical Research Center) for the generous gifts of SAB-132 and SAB-139 purified antibodies.

**Financial support.** This work was supported by the US Food and Drug Administration Office of Counterterrorism and Emerging Threats (OCET) - Medical Countermeasures initiative (MCMi) funds (OCET 2015910; to S. K.). This work was also funded in part by the Defense Threat Reduction Agency under interagency order HDTRA1826084 (to S. K.).

**Potential conflicts of interest.** All authors: No reported conflicts of interest. All authors have submitted the ICMJE Form for Disclosure of Potential Conflicts of Interest.

## References

1. Wong G, Richardson JS, Pillet S, et al. Immune parameters correlate with protection against ebola virus infection in rodents and nonhuman primates. *Sci Transl Med* **2012**; 4:158ra46.
2. Holtsberg FW, Shulenin S, Vu H, et al. Pan-ebolavirus and pan-filovirus mouse monoclonal antibodies: protection against Ebola and Sudan viruses. *J Virol* **2016**; 90:266–78.
3. Howell KA, Qiu X, Brannan JM, et al. Antibody treatment of Ebola and Sudan virus infection via a uniquely exposed epitope within the glycoprotein receptor-binding site. *Cell Rep* **2016**; 15:1514–26.
4. Matsushita H, Sano A, Wu H, et al. Species-specific chromosome engineering greatly improves fully human polyclonal antibody production profile in cattle. *PLoS One* **2015**; 10:e0130699.
5. Kuroiwa Y, Kasinathan P, Choi YJ, et al. Cloned transchromosomal calves producing human immunoglobulin. *Nat Biotechnol* **2002**; 20:889–94.
6. Arabi YM, Balkhy HH, Hayden FG, et al. Middle East respiratory syndrome. *N Engl J Med* **2017**; 376:584–94.
7. Beigel JH, Voell J, Kumar P, et al. Safety and tolerability of a novel, polyclonal human anti-MERS coronavirus antibody produced from transchromosomal cattle: a phase 1 randomised, double-blind, single-dose-escalation study. *Lancet Infect Dis* **2018**; 18:410–8.
8. Silver JN, Ashbaugh CD, Miles JJ, et al. Deployment of transchromosomal bovine for personalized antimicrobial therapy. *Clin Infect Dis* **2018**; 66:1116–19.
9. Bounds CE, Kwilas SA, Kuehne AI, et al. human polyclonal antibodies produced through DNA vaccination of transchromosomal cattle provide mice with post-exposure protection against lethal Zaire and Sudan ebolaviruses. *PLoS One* **2015**; 10:e0137786.
10. Dye JM, Wu H, Hooper JW, et al. Production of potent fully human polyclonal antibodies against Ebola Zaire virus in transchromosomal cattle. *Sci Rep* **2016**; 6:24897.
11. Khurana S, Fuentes S, Coyle EM, Ravichandran S, Davey RT Jr, Beigel JH. Human antibody repertoire after VSV-Ebola vaccination identifies novel targets and virus-neutralizing IgM antibodies. *Nat Med* **2016**; 22:1439–47.
12. Khurana S, Suguitan AL Jr, Rivera Y, et al. Antigenic fingerprinting of H5N1 avian influenza using convalescent sera and monoclonal antibodies reveals potential vaccine and diagnostic targets. *PLoS Med* **2009**; 6:e1000049.
13. Khurana S, Verma N, Yewdell JW, et al. MF59 adjuvant enhances diversity and affinity of antibody-mediated immune response to pandemic influenza vaccines. *Sci Transl Med* **2011**; 3:85ra48.
14. Dye JM, Herbert AS, Kuehne AI, et al. Postexposure antibody prophylaxis protects nonhuman primates from filovirus disease. *Proc Natl Acad Sci U S A* **2012**; 109:5034–9.
15. Oswald WB, Geisbert TW, Davis KJ, et al. Neutralizing antibody fails to impact the course of Ebola virus infection in monkeys. *PLoS Pathog* **2007**; 3:e9.
16. Parren PW, Geisbert TW, Maruyama T, Jahrling PB, Burton DR. Pre- and postexposure prophylaxis of Ebola virus infection in an animal model by passive transfer of a neutralizing human antibody. *J Virol* **2002**; 76:6408–12.
17. Wilson JA, Hevey M, Bakken R, et al. Epitopes involved in antibody-mediated protection from Ebola virus. *Science* **2000**; 287:1664–6.
18. Davidson E, Bryan C, Fong RH, et al. Mechanism of binding to Ebola virus glycoprotein by the ZMapp, ZMab, and MB-003 cocktail antibodies. *J Virol* **2015**; 89:10982–92.
19. Wec AZ, Herbert AS, Murin CD, et al. Antibodies from a human survivor define sites of vulnerability for broad protection against Ebolaviruses. *Cell* **2017**; 169:878–90 e15.
20. Zhao X, Howell KA, He S, et al. Immunization-elicited broadly protective antibody reveals Ebolavirus fusion loop as a site of vulnerability. *Cell* **2017**; 169:891–904 e15.